SolarPACES 2024, 30th International Conference on Concentrating Solar Power, Thermal, and Chemical Energy Systems

Measurement Systems, Devices, and Procedures

https://doi.org/10.52825/solarpaces.v3i.2402

© Authors. This work is licensed under a Creative Commons Attribution 4.0 International License

Published: 25 Nov. 2025

Enhanced On-Site Characterization of Heliostat Surface via Direct Calculation of Reflected Beam's Normal Vectors

SolarPACES 2024 Conference

Kontxi I. Aginaga Etxamendi^{1,*} , Angel M. Andueza^{2,3} , Adrian Peña-Lapuente¹, Sonia Escorza¹, and Marcelino Sanchez¹

¹CENER (National Renewable Energy Centre of Spain) ,Navarra, Spain

²Public University of Navarra, Pamplona, Navarra, Spain

³Smart Cities Institute, Public University of Navarra, Spain

*Correspondence: Kontxi I. Aginaga Etxamendi, kiaginaga@cener.com

Abstract. In this study, the results obtained through the algorithm presented for calculating the surface error will be analyzed. This aims to achieve a more precise characterization of the heliostat surface, independent of external conditions such as environment or solar field configuration. This can be accomplished by acquiring data obtained through HelioscharPlus characterization system, which has been presented in previous works and is distinguished by being based on data measured in real conditions, providing insights into the actual operation of the heliostat. This measurement mode offers the possibility to apply refinement process to the results, crucial for enhancing the accuracy of the characterization and aligning it more closely with real-world conditions.

Keywords: Helioscharplus, Temporal Constraints, Spatial Constraints, Normal Vectors

1. Introduction

In solar-thermal energy, among the essential performance parameters that define a heliostat, the optical quality is highly significant as it indicates how effectively the heliostat concentrates light onto the receiver. In this context Helioscharplus characterization system was designed, previously described in [1] publication. This characterization system consists of an array of cameras and detectors distributed along a pole or tower. The fundament of HelioscharPlus system is based on the use of the movement of the sun as a scanning element for scanning the heliostat reflected light beam through the detectors and cameras, maintaining the heliostat immobile. This system offers the unique ability to simultaneously characterize both the flux of the heliostat's reflected beam and its surface. Previous works have demonstrated its functionality through results from different testing campaigns, highlighting advantages in surface characterization over standards methods with high-resolution optical measurements[1], [2].

This work focuses on delving into the heliostat surface characterization to establish an approach that leads to the development of a more versatile characterization system. This system is intended to be applied in any environment under any condition, with the goal of obtaining more accurate results than those using standard surface characterization methodologies such

as deflectometry and photogrammetry. The main objective of this study is to analyze the results obtained through a different approach for calculating the surface error, aiming to achieve a more precise characterization of the heliostat surface independent of external conditions such as environment or solar field configuration.

2. Surface Normal Vector Calculation Algorithm

A complex algorithm is presented, designed to calculate the normal vector of each point on the heliostat surface using images of the heliostat. Through this algorithm, high precision can be achieved in characterizing the heliostat surface, as it enables an accurate reconstruction of its surface's geometry. This characterization methodology stands out for being based on data measured in real conditions, providing insights into the actual operation of the heliostat.

The algorithm uses data obtained through the Helioscharplus system [1], based on scanning the reflected light beam by the heliostat using cameras and detectors. This facilitates the possibility to obtain measurements of the time it takes for the reflected beam of light to sweep the system, providing valuable information about the heliostat's performance under specific measurement conditions.

Analyzing the images taken during the beam scanning, the algorithm is based on the optical configuration of the cameras, ensuring that the illuminated area on the heliostat surface in the images corresponds to the region reflecting direct sunlight onto the camera. This way in this work the incident vector is referred to the rays that came from the sun and falls to the heliostat surface and the reflected vector is referred to the ray that come from the heliostat surface and because surface reflective properties directs the light in another direction than the one it hits the surface direction. Therefore, knowing the sun's position at a specific location and time, the positions of the heliostat point and the camera, the incident and reflected vectors for each point on the heliostat can be determined. By applying the law of reflection, the normal vector direction relative to the incident and reflected light vectors is determined.

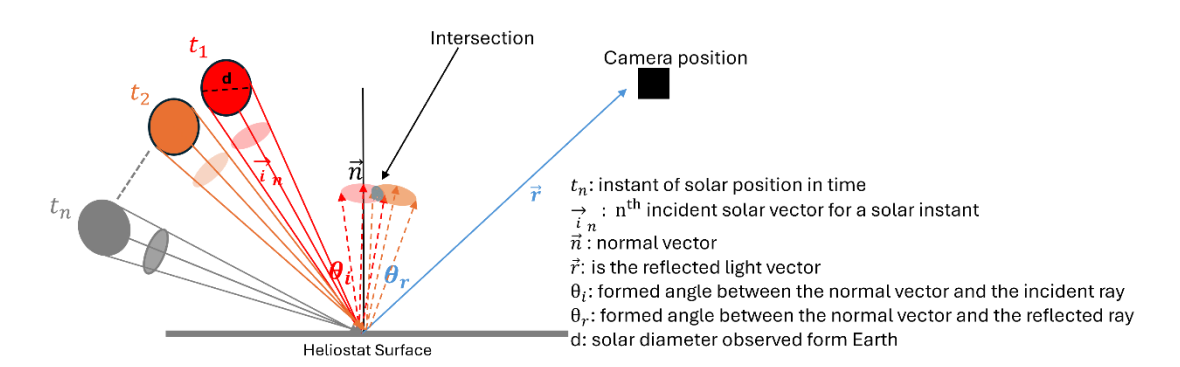


Figure 1. Diagram of Incidence, Reflection, and Normal Vectors that hits in a surface point with intersection Areas on a Surface

As an innovative approach, this algorithm considers the potential incident rays originating from the sun, taking into account the solar diameter as observed from Earth, that could intersect at the same moment for each point, as illustrated in *Figure 1* [3]. This results in a collection of multiple normal vectors identified for each point at every analyzed moment. To ensure that the obtained values closely approximate reality, restrictions are applied to this set of normal vectors. These limitations depend on the number of cameras used (spatial restriction) and the duration of the heliostat beam scan (temporal restriction), making them contingent on the system configuration and external factors, such as environmental conditions.

2.1 Temporal constraint

This constraint is related to the duration of the heliostat's reflected beam scan. As can be seen in *Figure 1*, at each instant in which an image related to the position of the sun is acquired, there are several solar vectors incident on the surface, which will lead to the calculation of a set of possible normal vectors for that surface. This calculation can be made using Snell's law, since, by knowing the position of the camera and whether the beam reflected by the heliostat is pointed towards it, the reflected ray can be determined. This will give rise to different sets of normal vectors corresponding to each camera and each instant of time, in which there will be common normal vectors at the consecutive intersections of both sets.

The diagram in *Figure 2.a* describes the procedure by which the algorithm applies the time constraint to the sets of normal vectors calculated for each point on the surface. The normal vectors of each heliostat point at each instant, when an image is taken, are calculated and analyzed, and these are compared with the set of normal vectors for the corresponding instant. Next, the intersection between the sets of the first and second instants is determined, selecting only the normal vectors that belong to this intersection. This process applies to the arrays of all cameras present in the system. Once the normal vectors of the intersection have been selected, this new subset is analyzed with the next instant, iterating in this way until all the images (all instants of time) of that point on the surface have been analyzed. The same procedure is then repeated for the next point on the surface.

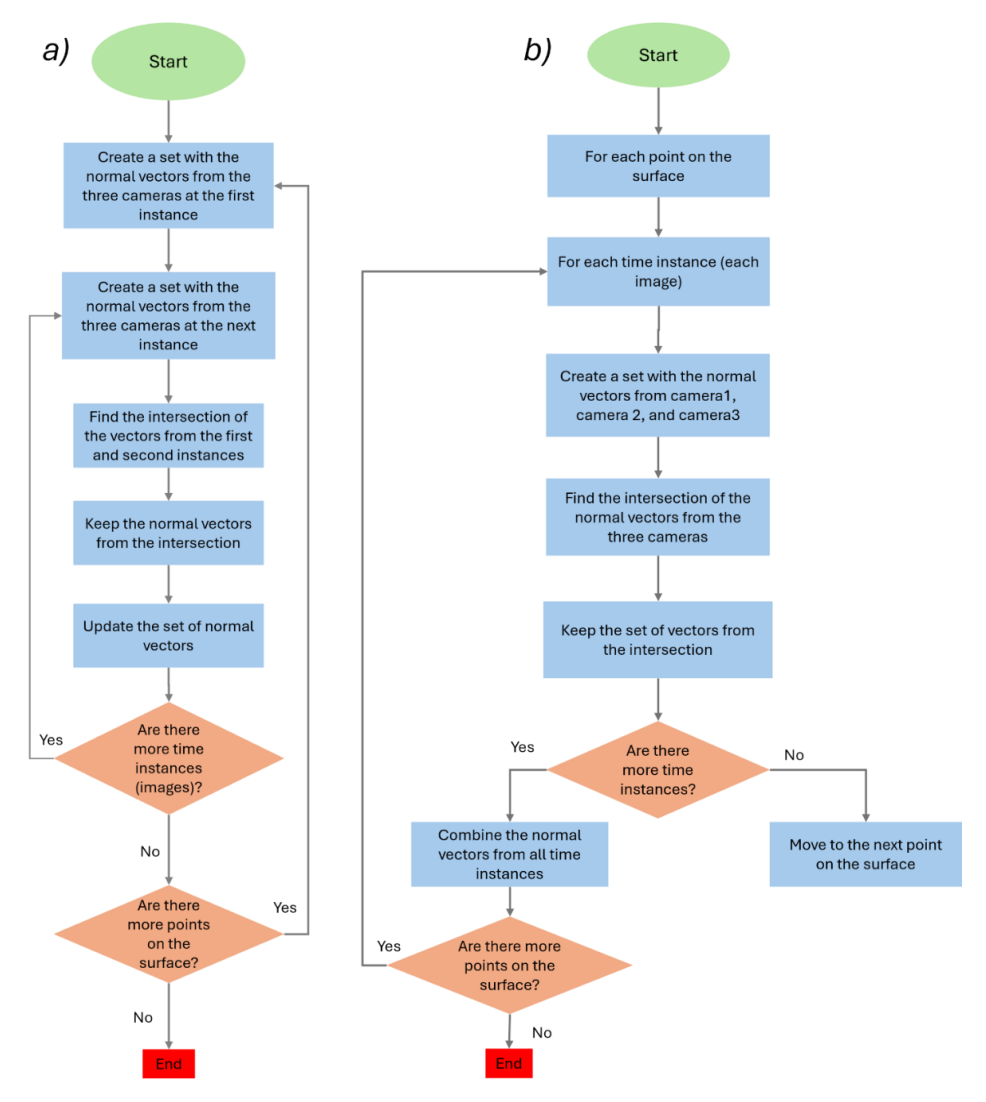


Figure 2. Flowchart explaining the algorithms that apply the constraints to the set of normal vectors. a) Flowchart of the temporal constraint algorithm. b) Flowchart of the spatial constraint algorithm.

2.2 Spatial constraint

This constraint is called special because it depends on the positions of the cameras (see **Figure 3**).

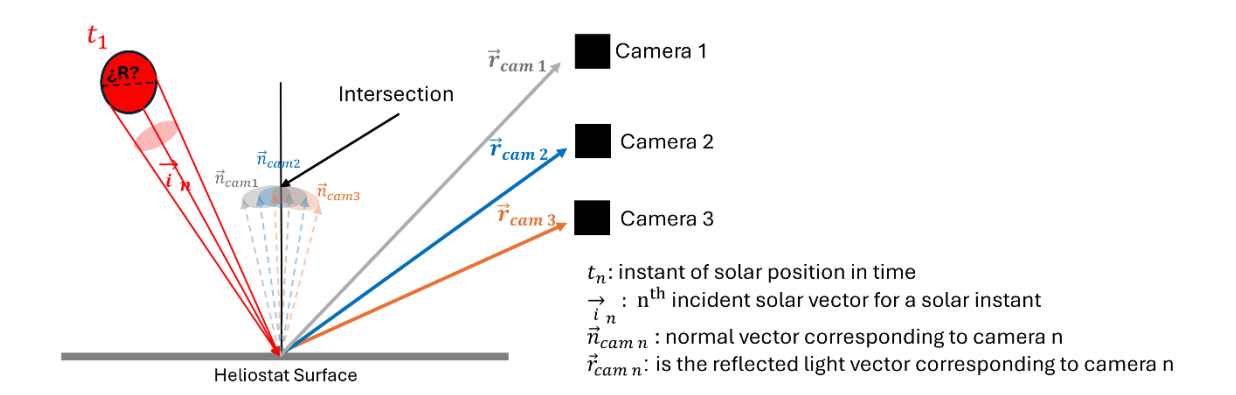


Figure 3. Diagram of the incidence, reflection, and normal vectors with intersection areas on a surface corresponding to the position of each camera.

The diagram in *Figure 2.b* illustrates the procedure by which the algorithm applies spatial constraint to the sets of normal vectors calculated for each instant of time on the surface of the heliostat. For each point on the surface, the normal vectors obtained at different times, identified by the system's cameras, are analyzed. Thus, for each point at any given moment, as many sets of normal vectors will be generated as there are cameras present in the system. The intersection of these camera arrays is then determined for each point at each instant of time. This resulting set is preserved to be applied to the next instant of time. The process is repeated until the analysis of all the instants of time is completed, and then the next point on the surface is carried out. This approach ensures that only vectors that are present in all cameras are considered, optimizing the accuracy of the analysis.

Once the spatial and temporal constraints have been applied to the normal vector sets of each point on the surface, only those vectors that match both constraints are selected. This results in an even smaller set of normal vectors for each point on the surface. This process of refinement by applying both constraints is crucial to improve the accuracy of the characterization and align it more closely with real-world conditions.

Finally, the angle of difference (Slope deviation) is calculated for each point on the surface, between the normal vectors that have been subjected to the constraints and the ideal normal vector corresponding to that point.

3. Experimental set-up

As detailed in the publication [1], the data were obtained at CENER's heliostat testing facility, located in Tudela de Navarra, Spain. As mentioned in the publication and the previous section, there is the Helioscharplus equipment system, which consists of a mast of 7.5 meters in length, with an active length of 6 meters, equipped with 24 optoelectronic photodetectors evenly distributed along the mast and an opening angle of the detectors of 7°, plus 3 cameras concentrated in the central section of the mast

The heliostat to be analyzed is a reference heliostat designed to be robust and flexible, the same one shown in the publication [1]. This heliostat is located 200 meters south of the system and is composed of 9 flat mirrors (facets) arranged in a 3 x 3 distribution. Each mirror is a silver second surface mirror, with an area of 1 m² and a thickness of 4 mm. The spherical

shape of the mirrors is achieved using 5 support points per mirror: one in the center and four more offset towards each corner. This configuration allows the shape and angle of inclination of the mirror to generate a reflective surface that forms a section of a sphere with a radius of 400 meters.

The data to which the algorithm's processing will be applied corresponds to a series of measurements carried out at that facility on May 17, 2022, during which the environmental conditions were optimal, with no clouds and low wind speed. The measurements were carried out between 1:39 p.m. and 1:45 p.m., around solar noon, when the height of the sun was 67.93°.

As explained in the publication [1], the measurement is done by keeping the heliostat stationary during data collection, which ensures a uniform and constant scan, without steps or deviations. This method is based on the movement of the sun as a scanning element of the light beam.

The data format for processing the measurements consists of monochromatic images of the heliostat captured by each camera at each instant of time, as the reflected beam sweeps across the system due to solar movement. Thus, the reflected beam scans the system made up of detectors and cameras, recording the intensity of the beam at all times and capturing images every second during the scan.

The test begins by orienting the heliostat in a position where its reflected beam does not reach the system. As the sun moves, the beam approaches the system until the scan is complete.

Once the beam has completely swept the system, images are taken with the cameras, increasing the exposure time to obtain photographs of the heliostat in diffused light. This will allow to use these images to detect the corresponding facets.

4. Results

This section shows the results obtained after applying the algorithm described above on the set of data acquired in the tests carried out explained in the experimental set-up section.

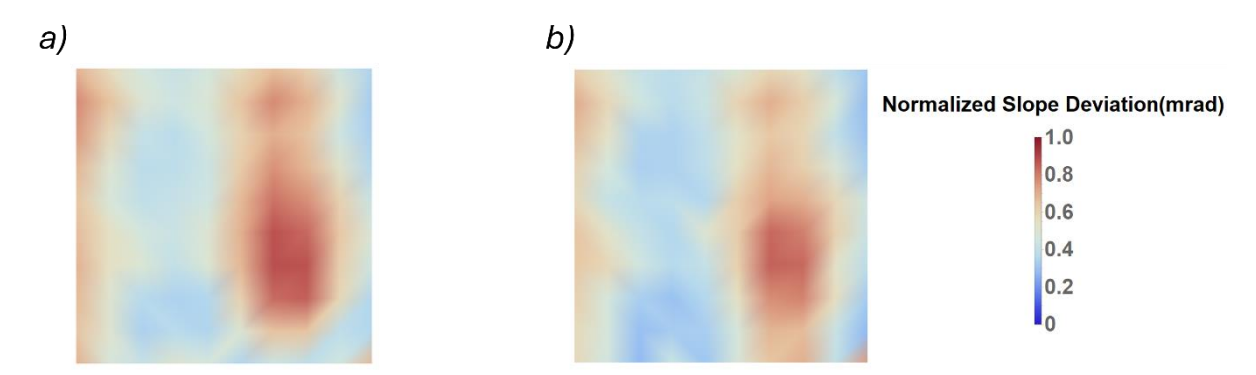


Figure 4. Figures Displaying SD calculations in a facet: a) without any imposed constraints. b) applying spatial and temporal constraints

Figure 4 shows the slope deviation obtained at each point on the surface of one of the facets that make up the heliostat. In these results, the average of all the slope deviations of the points of the facet has first been calculated, and then this average value has been subtracted from each point, which allows the changes to be observed more clearly. Thus, Figure 4.a shows the slope deviation obtained without applying any constraint on the calculated normal vectors, while Figure 4.b shows the slope deviation obtained after calculating the normal

vectors, after applying the temporal and spatial constraints; that is, only the set of normal vectors present after applying both constraints is considered.

In the results obtained from *Figure 4* it can be seen that, in both cases, a similar result is obtained in the deviation of the slope of the surface. However, when applying constraints, it is noticeable how especially the area that appears with a higher red value is sharper, there is greater variation in slope deviation. Some areas of the heliostat surface, which had initially been detected as areas of low slope deviation, actually show a higher value of deviation after applying the constraints. This is clearly seen in the lower section of the facet. The same happens the other way around, where areas of the surface that a priori were observed with a high value of slope deviation after applying the constraints it is observed that in reality the value is lower, observed in the upper right part of the facet. This indicates that, in the image where constraints are applied, greater precision is achieved in gradient changes from a point on the surface to the adjacent point.

Figure 5 below illustrates the results of Slope Deviation (SD) on all facets of the heliostat, obtained from the algorithm with and without constraints imposed on the calculation of the normal surface vector.

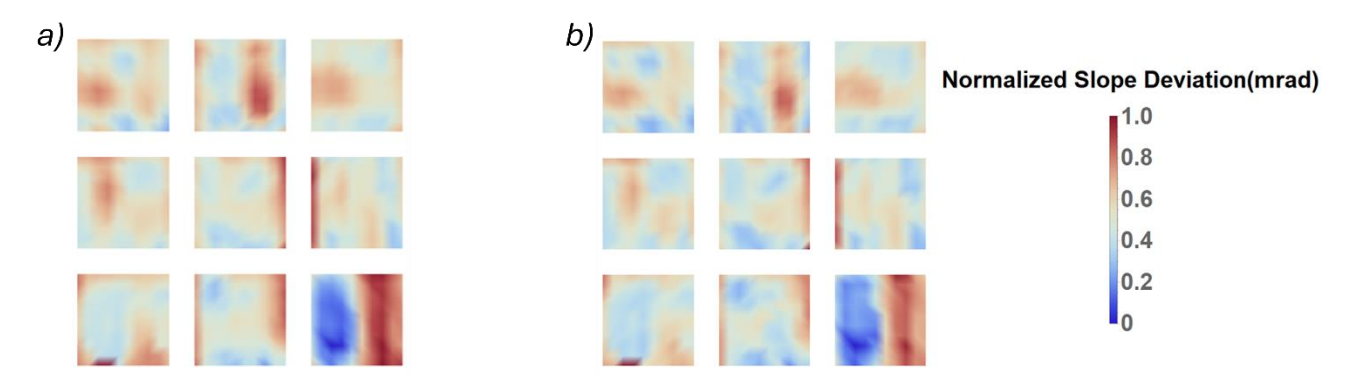


Figure 5. Figures Displaying SD calculations in a complete heliostat: a) without any imposed constraints. b) applying spatial and temporal constraints

The results show that, both with and without constraints, the slope deviation obtained on the surface of the heliostat is very similar.

Importantly, in *Figure 5*, the lower right facet shows considerable slope deviation. This is because when the tests were carried out, it was detected that this facet had slack. This indicates a defect in the facet, which is slightly loose compared to the structure. On the other hand, there are areas, such as at the bottom of the lower left facet, where certain spots never light up. As a result, they are assigned the maximum slope deviation value, as that area should reflect the heliostat beam back to the camera, but due to optical distortions it does not.

As with single-facet analysis, applying constraints to all facets of the heliostat allows for more accurate observation of slope deviation values in each area of the surface.

5. Conclusions

The results, which show a heat map of slope deviation values in a facet of the heliostat, provide an approximation of the behavior of the rays reflected on the surface. These results provide insight into optical distortions, which can be caused by environmental conditions (such as temperature and humidity) as well as surface imperfections.

On an ideal surface (under optimal conditions and without damage), it would be observed that the facet would have a uniform slope deviation color or value throughout its area. In this

way, the inhomogeneities observed in the facet allow us to interpret that, if a facet is poorly edged to a certain side, all its normal vectors will also show a deviation to that side, reflecting a slope deviation according to that incorrect inclination.

These surface errors affect the efficiency of solar plants, as maximum deflection at all points results in a proportional deflection in reflected light. For example, in the facilities that have been measured, a slope deviation of 1 mrad would mean a beam deviation of 0.2 meters at 200 meters. Therefore, consequently, obtaining more accurate information about the optical behavior of the heliostat surface is essential for increasing the energy efficiency of solar thermal tower plants.

In this way, this tool, which applies restrictions considering the period during which the data was collected and the configuration of the system, allows any heliostat to be analyzed regardless of the conditions under which it operates, providing precise information about the optical behavior of the heliostat. The implementation of this methodology in commercial plants will not only enable continuous monitoring of the optical quality of the heliostats, but also link this quality to their geometry and mechanical operating conditions. This will provide valuable insights for developing precise procedures and actions in operations and maintenance tasks, ensuring that the heliostat fields remain in optimal working condition throughout their operational lifespan.

6. Future work

A deeper analysis of the combined optical, geometric, and mechanical aspects remains pending. This is necessary to establish practical recommendations and actions that can enhance the optical quality of heliostats throughout their lifespan, from installation and commissioning to routine operation. The ultimate goal is to develop a procedure based on this knowledge, providing maintenance personnel with precise instructions to improve the optical performance of heliostats as soon as any deviation from their design behavior is detected. This could involve setting guidelines for adjustments, specifying not only which mirror facets to address but also which specific fasteners (bolts, nuts, washers, etc.) to act upon, and how to do so to correct the identified deviations.

Data availability statement

For more information about the data used, contact the authors.

Author contributions

Study design: M .Sanchez, A .M. Andueza

Data Collection: K.I. Aginaga Etxamendi, S. Escorza, A. Peña-Lapuente

Data analysis: K.I. Aginaga Etxamendi, , S. Escorza, A. Peña-Lapuente

Software: Kontxi I. Aginaga Etxamendi

Writing-Original draft: Kontxi I. Aginaga

Project Supervision: M .Sanchez, A .M. Andueza

Writing-Review & Editing: M .Sanchez, A .M. Andueza, A. Peña-Lapuente

Technical Contributions: I.D Bernard

Competing interests

The authors declare that they have no competing interests

Funding

This work is part of the action PCI2022-135015-2, funded by MCIN/AEI/10.13039/501100011033 and by the European Union "NextGenerationEU"/PRTR.

References

- [1] A. Peña *et al.*, "Novel scanner-based methodology for a fast and complete high quality characterization of all solar field heliostats, their facets, and corresponding reflected beams," p. 3, 2023, doi: 10.1117/12.2677246
- [2] A.Peña-Lapuente *et al.*, "Initial validation of an advanced heliostat characterizationsystembased on cameras and light detectors," *AIP Conf. Proc.*, vol. 2445, 2022, doi: 10.1063/5.0085728
- [3] J. Yan, Z. R. Cheng, and Y. D. Peng, "Effect of tracking error of double-axis tracking device on the optical performance of solar dish concentrator," *Int. J. Photoenergy*, vol. 2018, 2018, doi: 10.1155/2018/9046127